AIP | The Journal of Chemical Physics

Unraveling the success and failure of mode coupling theory from consideration of entropy

Manoj Kumar Nandi, Atreyee Banerjee, Shiladitya Sengupta, Srikanth Sastry, and Sarika Maitra Bhattacharyya

Citation: The Journal of Chemical Physics **143**, 174504 (2015); doi: 10.1063/1.4934986
View online: http://dx.doi.org/10.1063/1.4934986
View Table of Contents: http://scitation.aip.org/content/aip/journal/jcp/143/17?ver=pdfcov
Published by the AIP Publishing

Unraveling the success and failure of mode coupling theory from consideration of entropy

Manoj Kumar Nandi,[1,a)] Atreyee Banerjee,[1,a)] Shiladitya Sengupta,[2] Srikanth Sastry,[3] and Sarika Maitra Bhattacharyya[1,b)]
[1]*Polymer Science and Engineering Division, CSIR-National Chemical Laboratory, Pune 411008, India*
[2]*Department of Chemical Physics, Weizmann Institute of Science, Rehovot 76100, Israel*
[3]*Theoretical Sciences Unit, Jawaharlal Nehru Centre for Advanced Scientific Research, Jakkur Campus, Bengaluru 560 064, India*

(Received 30 June 2015; accepted 19 October 2015; published online 6 November 2015)

We analyze the dynamics of model supercooled liquids in a temperature regime where predictions of mode coupling theory (MCT) are known to be valid qualitatively. In this regime, the Adam-Gibbs (AG) relation, based on an activation picture of dynamics, also describes the dynamics satisfactorily, and we explore the mutual consistency and interrelation of these descriptions. Although entropy and dynamics are related via phenomenological theories, the connection between MCT and entropy has not been argued for. In this work, we explore this connection and provide a microscopic derivation of the phenomenological Rosenfeld theory. At low temperatures, the overlap between the MCT power law regime and AG relation implies that the AG relation predicts an avoided divergence at T_c, the origin of which can be related to the vanishing of pair configurational entropy, which we find occurring at the same temperature. We also show that the residual multiparticle entropy plays an important role in describing the relaxation time. © *2015 AIP Publishing LLC.* [http://dx.doi.org/10.1063/1.4934986]

I. INTRODUCTION

In the study of liquid state physics, the structure of the liquid, which is often described primarily by the two body radial distribution function (rdf), has always played a central role. The structure cannot only describe the thermodynamic properties of the liquid like the energy and pressure, under certain theoretical framework like the mode coupling theory the structure can also determine the dynamics.[1,2] In a series of papers, Berthier and Tarjus have described the behaviour of two systems with different interaction potentials, namely, the Lennard-Jones (LJ) and the Weeks-Chandler-Andersen (WCA) potentials. Although at the same temperature and density, the structures of these systems are very close, the dynamics display significant differences at low temperatures.[3–6] These studies questioned the role of structure in determining the dynamics. Coslovich has shown that although the two body radial distribution function of these two systems are quite similar, the triplet correlations are significantly different.[7] He has also shown that the LJ system has more pronounced local ordering.[8] In supercooled liquids, these locally preferred structures are known to form correlated domains which have been argued to give rise to the slow dynamics.[9] An estimation of this length scale of the domains and its connection to the relaxation time scale is a topic of ongoing research.[10,11] One such study by Hocky *et al.* has shown that the point-to-set correlation length of the LJ system is larger compared to that of the WCA system and this difference in correlation length can account for the difference in dynamics of the two systems.[12] From these studies, one may conclude that the difference in dynamics primarily comes from many body correlations. However, in one of our recent study, it has been shown that two body correlation information is good enough to capture the difference in the dynamics between the two systems. The study also reveals that the temperature at which an approximation to the configurational entropy using pair correlation alone goes to zero, is similar to the mode coupling theory (MCT) transition temperature, T_c.[13] As mentioned before, MCT is a microscopic theory where the structural inputs determine the dynamics. Although entropy and dynamics are related *via* phenomenological Rosenfeld[14] and Adam-Gibbs (AG)[15] relations at high and low temperatures, respectively, MCT does not have any apparent connection to entropy. Thus, it is of great interest to try to understand the origin of the coincidence of the MCT divergence temperature and the temperature where pair configurational entropy goes to zero.

At normal liquid temperatures, a semi-quantitative correlation between the dynamics (transport properties) and thermodynamics (excess entropy), proposed by Rosenfeld,[14,16] has been extensively studied in recent times, where the relaxation time τ can be written as

$$\tau(T) = C \exp\left[-K S_{ex}\right]. \tag{1}$$

Here, C and K are constants. Since the pair entropy S_2, which is obtained only from the pair correlation function, accounts for 80%–90% of the excess entropy,[13,17] many simulation studies have replaced S_{ex} by S_2 and have shown that even with S_2, the transport coefficients follow Rosenfeld scaling.[6,18–21]

Bagchi and coworkers used Zwanzig's rugged energy landscape model of diffusion[22] and by connecting the

a)M. K. Nandi and A. Banerjee contributed equally to this work.
b)Electronic mail: mb.sarika@ncl.res.in

ruggedness to the excess entropy have provided a derivation of Rosenfeld relation.[23] Samanta *et al.*[24] have shown that under certain approximations the diffusion coefficient as obtained from MCT follows Rosenfeld scaling. Das and coworkers have performed microscopic MCT calculations which show that the diffusion values thus obtained can be fitted to Rosenfeld scaling.[25] Some of these studies have reported that the scaling parameter is not unique; hence, the whole temperature region cannot be fitted to a single straight line.[25,26]

Although Rosenfeld scaling holds at high temperatures, it is known to breakdown at low temperatures even with multiple scaling parameters. At low temperatures, the correlation between the transport coefficients and entropy is usually described by the well known Adam-Gibbs relation,[15]

$$\tau(T) = \tau_o \exp\left(\frac{A}{TS_c}\right), \tag{2}$$

where S_c is the configurational entropy of the system. For a wide range of systems, the AG relation is found to hold[13,27,28] below a moderately high temperature referred to as the onset temperature of slow dynamics.

In this paper, we explore the connection between dynamics, characterization of structure as contained in the pair and higher order correlations, and entropy, and relations between them as described by the MCT and the AG relation, using computer simulations of two model liquids and analytical results that seek to relate descriptions of dynamics in terms of structure, and entropy. Our present study shows that the AG theory, which is based on activation dynamics can completely describe the MCT power law behaviour in the region where the latter is found to be valid. An earlier study which observed a similar overlap region[29] argued that the observation supports the hypothesis that a direct relation exists between the number of basins and their connectivity.[30,31]

There has also been a recent study[32] where the configurational entropy is evaluated by considering the effective potential between the coupled replicas of two model liquids, and the observed shrinking of the domain of validity of the AG relation is claimed to be a parallel observation based on experimental data,[33,34] which appears not to be a related observation upon closer inspection. Experimentally, the configurational entropy is estimated through the excess entropy over the crystal, and in Ref. 34 it was shown that the ratio of the configurational heat capacity to the excess heat capacity increases with a decrease of the fragility. In turn, it was shown in Ref. 33 that less fragile liquids show a closer conformity with the Adam-Gibbs relation at high temperatures. Thus, the conclusion that could be derived from the experimental studies is that a proper subtraction of the vibrational component of the entropy would lead to better agreement with the Adam-Gibbs relation. This is indeed what is achieved in the procedure we employ here, and a large number of simulation studies[29,35–44] using procedures similar to ours show impressive ranges of temperatures over which the Adam-Gibbs relation is valid. Thus, the implications of the results[32] remain to be properly understood. Further, the observation in Ref. 33 was that the linear dependence of the TS_c, required to obtain the Vogel-Fulcher-Tammann (VFT) temperature dependence via the Adam-Gibbs relation, was valid over the range of temperatures studied, but the relaxation times showed deviations from the VFT form. For the systems studied in the present work, the linear temperature dependence of TS_c is observed in the temperature range studied, and the relaxation times are found as well to obey the VFT temperature dependence. But we also find a temperature window of overlap where both the Adam-Gibbs and VFT form, as well as the power law dependence predicted by MCT, appear valid. In order to understand this observation, we explore the connection between MCT and entropy and discuss different predictions of MCT in the light of entropy.

Although MCT makes predictions about dynamics in both Rosenfeld and AG temperature regimes, no connection between MCT and entropy has been argued for, except for one study,[24] as mentioned earlier. We show that, under some assumptions, the memory function in the MCT equation for structural relaxation is related to the pair excess entropy, thus providing a microscopic derivation of the phenomenological Rosenfeld expression for the structural relaxation time, τ. Our study also can explain the origin of the temperature dependence of the Rosenfeld parameter. Earlier studies have shown that the relaxation time as obtained from simulation is smaller and have lower activation energy when compared to that predicted by MCT using the structural information from the simulations.[4,45] Our analysis of the memory function can explain this behaviour.

As mentioned above, the AG relation is valid for a wide temperature range which includes the range in which the MCT power law prediction holds. Thus, in the MCT regime, the relaxation time follows both the AG and MCT behaviours. Our study reveals that the origin of the avoided divergence-like behaviour (as given by MCT power law) in the AG relation is related to the vanishing of the pair configurational entropy. For all the systems studied here, the pair configurational entropy is found to vanish close to the MCT transition temperature T_c. Although we find an empirical evidence of the coincidence of these two temperatures, in the present study, we have not been able to establish a causal relationship between them. We also show that the pair configurational entropy via the AG relation, although predicts the correct MCT transition temperature, by itself cannot predict the MCT power law behaviour. The RMPE plays an important role in providing the correct temperature dependence of relaxation times. We also find a connection between the AG coefficient (A), pair thermodynamic fragility (K_{T2}) and MCT critical exponent (γ). We show that although both "A" and K_{T2} are dependent on density, their ratio which is related to γ is density-independent.

The paper is organized as follows: The simulation details are given in Sec. II. In Sec. III, we describe the methods used for evaluating the various quantities of interest and provide other necessary background. In Sec. IV, we report some observations that motivate our analytical results which are described in Sec. V. In Sec. VI, we present additional numerical results and their analysis. Sec. VII contains a discussion of presented results and conclusions.

II. SIMULATION DETAILS

We have simulated the Kob-Andersen model which is a binary mixture (80:20) of LJ particles and the corresponding WCA version.[46,47] The interatomic pair potential, $U_{\alpha\beta}(r)$ between species α and β, where $\alpha, \beta = A, B$, is described by a shifted and truncated LJ potential, as given by

$$U_{\alpha\beta}(r) = \begin{cases} U_{\alpha\beta}^{(LJ)}(r;\sigma_{\alpha\beta},\epsilon_{\alpha\beta}) - U_{\alpha\beta}^{(LJ)}(r_{\alpha\beta}^{(c)};\sigma_{\alpha\beta},\epsilon_{\alpha\beta}), & r \le r_{\alpha\beta}^{(c)} \\ 0, & r > r_{\alpha\beta}^{(c)} \end{cases}, \tag{3}$$

where $U_{\alpha\beta}^{(LJ)}(r;\sigma_{\alpha\beta},\epsilon_{\alpha\beta}) = 4\epsilon_{\alpha\beta}[(\sigma_{\alpha\beta}/r)^{12} - (\sigma_{\alpha\beta}/r)^{6}]$ and $r_{\alpha\beta}^{(c)} = 2.5\sigma_{\alpha\beta}$ for the LJ systems and $r_{\alpha\beta}^{(c)}$ is equal to the position of the minimum of $U_{\alpha\beta}^{(LJ)}$ for the WCA systems. Length, temperature, and time are given in units of σ_{AA}, k_BT/ϵ_{AA}, and $\tau = \sqrt{(m_A\sigma_{AA}^2/\epsilon_{AA})}$, respectively. Here, we have simulated Kob Andersen Model with the interaction parameters $\sigma_{AA} = 1.0$, $\sigma_{AB} = 0.8$, $\sigma_{BB} = 0.88$, $\epsilon_{AA} = 1$, $\epsilon_{AB} = 1.5$, $\epsilon_{BB} = 0.5$, $m_A = m_B = 1.0$.

The molecular dynamics (MD) simulations have been carried out using the LAMMPS package.[48] We have performed MD simulations in the canonical ensemble (NVT) using Nosé-Hoover thermostat with integration time step 0.005τ. The time constants for Nosé-Hoover thermostat are taken to be 100 time steps. The sample is kept in a cubic box with periodic boundary condition. System size is $N = 500$, $N_A = 400$ (N = total number of particles, N_A = number of particles of type A) and we have studied a broad range of density ρ from 1.2 to 1.6. For all state points, three to five independent samples with run lengths $>100\tau$ (τ is the α-relaxation time) are analysed.

III. DEFINITIONS AND BACKGROUND

A. Relaxation time

We have calculated the relaxation times from the decay of the overlap function q(t), using $q(t = \tau, T)/N = 1/e$. The overlap function is defined as

$$\begin{aligned} \langle q(t)\rangle &\equiv \left\langle \int dr\, \rho(r,t_0)\rho(r,t+t_0)\right\rangle \\ &= \left\langle \sum_{i=1}^{N}\sum_{j=1}^{N} \delta(\mathbf{r}_j(t_0) - \mathbf{r}_i(t+t_0))\right\rangle \\ &= \left\langle \sum_{i=1}^{N} \delta(\mathbf{r}_i(t_0) - \mathbf{r}_i(t+t_0))\right\rangle \\ &\quad + \left\langle \sum_{i}\sum_{j\neq i} \delta(\mathbf{r}_i(t_0) - \mathbf{r}_j(t+t_0))\right\rangle. \end{aligned} \tag{4}$$

The overlap function is a two-point time correlation function of local density $\rho(r,t)$. It has been used in many recent studies of slow relaxation.[27] In this work, we consider only the self-part of the total overlap function (i.e. neglect the $i \neq j$ terms in the double summation) as the dependence of the relaxation time on temperature or density is similar both for self- and full overlap function.

So, the self-part of the overlap function can be written as

$$\langle q(t)\rangle \approx \left\langle \sum_{i=1}^{N} \delta(\mathbf{r}_i(t_0) - \mathbf{r}_i(t+t_0))\right\rangle. \tag{5}$$

The δ function is approximated by a window function $\omega(x)$ which defines the condition of overlap between two particle positions separated by a time interval t,

$$\begin{aligned} \langle q(t)\rangle &\approx \left\langle \sum_{i=1}^{N} \omega(|\ \mathbf{r}_i(t_0) - \mathbf{r}_i(t+t_0)\ |)\right\rangle \\ \omega(x) &= 1, x \le \text{a implying overlap} \\ &= 0, \text{otherwise.} \end{aligned} \tag{6}$$

The time dependent overlap function thus depends on the choice of the cutoff parameter a, which we choose to be 0.3. This parameter is chosen such that particle positions separated due to small amplitude vibrational motion are treated as the same, or that a^2 is comparable to the value of the MSD in the plateau between the ballistic and diffusive regimes.

Relaxation times have been obtained from the decay of the self-intermediate scattering function $\phi_s(k,t)$ using the definition $\phi_s(k, t = \tau, T) = 1/e$ at $k \simeq 2\pi/r_{max}$, where r_{max} is the first maximum of the radial distribution function. The self-intermediate scattering function is calculated from the simulated trajectory as

$$\phi_s(k,t) = \frac{1}{N}\left\langle \sum_{i=1}^{N} \exp\left(-i\mathbf{k}.(\mathbf{r}_i(t) - \mathbf{r}_i(0))\right)\right\rangle. \tag{7}$$

Since the relaxation times obtained from $q(t)$ and $\phi_s(k,t)$ behave very similarly, for the low temperature calculation which requires longer time averaging, to save computational time we have used the time scale obtained from $q(t)$.

B. Static structure factor

The partial structure factors $S_{\alpha\beta}(k)$, needed as input for the MCT calculations, can be defined as

$$S_{\alpha\beta}(k) = \frac{1}{\sqrt{N_\alpha N_\beta}} \sum_{i=1}^{N_\alpha}\sum_{j=1}^{N_\beta} \exp\left(-i\mathbf{k}.(\mathbf{r}_i^\alpha - \mathbf{r}_j^\beta)\right). \tag{8}$$

C. Mode coupling theory

Many properties of glass forming liquids can be explained by the well known MCT. This microscopic theory can give a qualitative description of dynamical properties (such as

temperature dependence of relaxation time) if the static structure of the liquid is known and many experiments and simulation results have shown that MCT predictions hold good in the temperature regime of initial slow down of the dynamics.[2] The equation for the intermediate scattering function for the binary mixture is given by

$$\ddot{\boldsymbol{S}}(k,t) + \boldsymbol{\Gamma}\dot{\boldsymbol{S}}(k,t) + \boldsymbol{\Omega}^2(k)\boldsymbol{S}(k,t) + \boldsymbol{\Omega}^2(k)\int dt'\boldsymbol{\mathcal{M}}(t-t')\dot{\boldsymbol{S}}(k,t') = 0, \quad (9)$$

where $\boldsymbol{\Omega}^2(k) = \frac{k^2 k_B T}{m}\boldsymbol{S}^{-1}(k)$ and $\boldsymbol{S}(k,t)$ is the matrix of intermediate scattering functions $S_{\alpha\beta}(k,t)$ and the memory function $\boldsymbol{\mathcal{M}}$ can be written as

$$(\Omega^2(k)\mathcal{M}(k,t))_{\alpha\beta} = \frac{1}{2\rho\sqrt{x_\alpha x_\beta}}\sum_{ll'mm'}\int\frac{d\boldsymbol{q}}{(2\pi)^3} V_{\alpha lm}(\mathbf{q},\mathbf{k}-\mathbf{q})V_{\beta l'm'}(\mathbf{q},\mathbf{k}-\mathbf{q}) \times S_{mm'}(|\mathbf{k}-\mathbf{q}|)S_{ll'}(q) \phi_{mm'}(|\mathbf{k}-\mathbf{q}|,t)\phi_{ll'}(q,t), \quad (10)$$

where $\phi_{\alpha\beta}(k,t) = \frac{S_{\alpha\beta}(k,t)}{S_{\alpha\beta}(k,0)}$, $\mathbf{k}-\mathbf{q}=\mathbf{p}$, and $V_{\alpha lm}(\mathbf{q},\mathbf{p}) = [\hat{\mathbf{k}}.\mathbf{q}\delta_{\alpha m}C_{\alpha l}(q) + \hat{\mathbf{k}}.\mathbf{p}\delta_{\alpha l}C_{\alpha m}(p)]$; here, $\boldsymbol{C}(q)$ is defined as $\boldsymbol{S}^{-1}(q) = \mathbf{1} - \boldsymbol{C}(q)$. The static structure factor is obtained from computer simulation using Eq. (8).

Solving Eq. (9) we have calculated the relaxation times, $\tau_{\alpha\beta}$ from $\phi_{\alpha\beta}(q,t)$ at $1/e$ and the average relaxation time is obtained from the following equation:

$$\tau_{MCT} = \sum_{\alpha\beta} x_\alpha x_\beta \tau_{\alpha\beta}. \quad (11)$$

D. Configurational entropy

Configurational entropy (S_c per particle) is a measure of the number of distinct local energy minima. It is calculated[49] by subtracting the vibrational component from the total entropy of the system: $S_c(T) = S_{total}(T) - S_{vib}(T)$.[27,36] The total entropy for the binary mixture is obtained via thermodynamic integration from the ideal gas limit. Vibrational entropy for the binary mixture is calculated by making a harmonic approximation to the potential energy about a given local minimum.

E. Pair configurational entropy

To get an estimate of the configurational entropy as predicted by the pair correlation we rewrite S_c in terms of the pair contribution to configurational entropy S_{c2},[13]

$$S_c = S_{id} + S_{ex} - S_{vib} = S_{id} + S_2 + \Delta S - S_{vib} = S_{c2} + \Delta S. \quad (12)$$

S_{ex} can be expanded in an infinite series, $S_{ex} = S_2 + S_3 + \ldots = S_2 + \Delta S$ using Kirkwood's factorization[50] of the N-particle distribution function.[51–53] S_n is the "n" body contribution to the entropy. Thus, the pair excess entropy is S_2 and the higher order contributions to excess entropy is given by the residual multiparticle entropy (RMPE), $\Delta S = S_{ex} - S_2$.[54] The pair configurational entropy is written as $S_{c2} = S_{id} + S_2 - S_{vib}$. An expansion of S_{vib} in terms of two and many body would be interesting but to the best of our knowledge, this has not been attempted before. Thus, we have used total S_{vib}. The pair entropy S_2 for a binary system can be written in terms of the partial radial distribution functions,

$$\frac{S_2}{k_B} = -2\pi\rho\sum_{\alpha,\beta}x_\alpha x_\beta\int_0^\infty\{g_{\alpha\beta}(r)\ln g_{\alpha\beta}(r) - [g_{\alpha\beta}(r)-1]\}r^2dr, \quad (13)$$

where $g_{\alpha\beta}(r)$ is the atom-atom pair correlation between atoms of type α and β, N is the total number of particles, x_α is the mole fraction of component α in the mixture, and k_B is the Boltzmann constant.

IV. OBSERVATIONS

As the liquid is supercooled, the Rosenfeld scaling, observed to be valid at normal temperatures, is known to break down.[26] However, in this regime, the Adam-Gibbs relation is found to hold.[15,27] The Adam Gibbs relation explains the behaviour of dynamical property like relaxation time using configurational entropy which is a thermodynamical property. So this relation connects thermodynamics and dynamics for low temperature liquids. In the Adam-Gibbs relation, it is not the excess entropy but the configurational entropy which dictates the dynamics.

Although microscopic MCT shows a divergence of the relaxation time, τ, at a much higher temperature[55] than the glass transition temperature, the power law behaviour of τ as predicted by MCT is found to be valid in a range of low temperatures. Similar to the earlier studies,[4,45] the power law behaviour of simulated τ is well described by an algebraic divergence given by

$$\tau \sim (T - T_c)^{-\gamma} \sim \left(\frac{T}{T_c} - 1\right)^{-\gamma}. \quad (14)$$

For all the densities we study, as shown in Fig. 1, in a certain region of temperature, $(10^{-1} \le (\frac{T}{T_c} - 1) \le 10^0)$, the relaxation time, τ, for both LJ and WCA systems follow the MCT power law behaviour. On the other hand, the Adam Gibbs relation is also valid for all the systems in the region

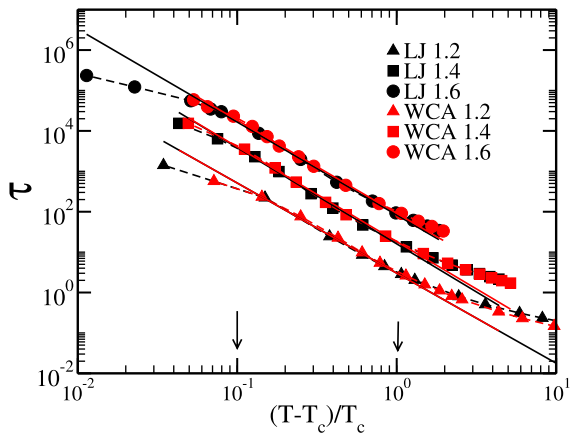

FIG. 1. The power law behaviour of relaxation times of numerical simulation, τ, as predicted by MCT (Eq. (14)) appears as a straight line for a certain region $(10^{-1} \le (\frac{T}{T_c} - 1) \le 10^0)$ for both the systems at all densities. The critical exponent γ is obtained from the slope of the linear fit. For clarity, data at different densities are vertically shifted.

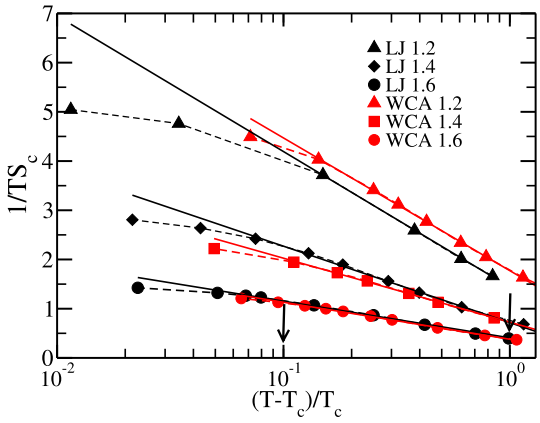

FIG. 2. $\frac{1}{TS_c}$ plotted against $(\frac{T}{T_c}-1)$ and as predicted by Eq. (15) the plots are linear in the region $10^{-1} \leq (\frac{T}{T_c}-1) \leq 10^{0}$ validating our claim that MCT power law regime overlaps with AG regime.

$(0 \lesssim (\frac{T}{T_c}-1) \leq 10^{0})$.[56] Thus, we find that the temperature range, where the MCT like behaviour is predicted, completely overlaps with the range where the Adam-Gibbs relation is found to be valid. As mentioned in the Introduction, this overlap regime has earlier been reported for other systems.[29] As in this temperature regime, τ_α can be described both by MCT power law behaviour and by the AG relation we can write

$$\frac{A}{TS_c} \propto -\gamma \ln(\frac{T}{T_c}-1). \tag{15}$$

In Fig. 2, we show that $\frac{1}{TS_c}$ is linear when plotted against $\ln(\frac{T}{T_c}-1)$ in the region $10^{-1} \leq (\frac{T}{T_c}-1) \leq 10^{0}$ validating the statement that MCT like divergence region overlaps with AG region.

Since the configurational entropy has a finite value at the MCT transition temperature, T_c, the AG relation is not expected to predict a divergent relaxation time at this temperature. In order to investigate the origin of this avoided transition, we consider the separation of the configurational entropy into pair and many body parts as described earlier (Sec. III E).[13] We find that the temperature dependence of (S_{c2}) is given by (Fig. 3)

$$TS_{c2} = K_{T2}(\frac{T}{T_{K2}}-1), \tag{16}$$

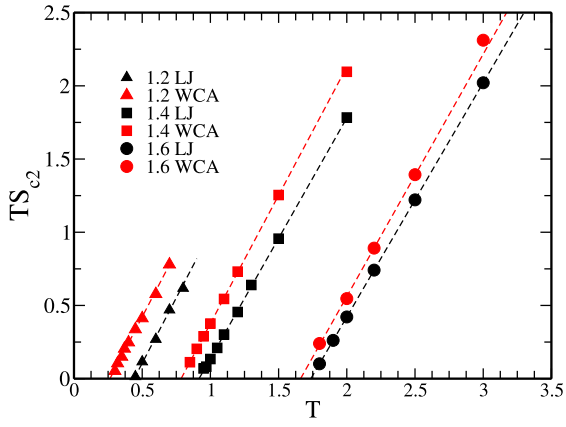

FIG. 3. The temperature dependence of pair configurational entropy (S_{c2}) to determine Kauzmann temperature T_{K2}. T_{K2} values are given in Table I.

TABLE I. T_c[6] and T_{K2} values are tabulated below. For all the systems studied here, the Kauzmann temperatures for S_{c2} are quite similar to the MCT transition temperatures.

	$\rho = 1.2$		$\rho = 1.4$		$\rho = 1.6$	
	T_c	T_{K2}	T_c	T_{K2}	T_c	T_{K2}
LJ	0.435	0.445	0.93	0.929	1.76	1.757
WCA	0.28	0.268	0.81	0.788	1.69	1.696

where K_{T2} is the pair thermodynamic fragility and S_{c2} vanishes at the Kauzmann temperature T_{K2}.[13] T_{K2} is obtained from the linear fit of TS_{c2} vs T plot at $S_{c2} = 0$. As reported earlier, we find that for all the systems studied in this work, the Kauzmann temperature for S_{c2} is very close in value to the MCT transition temperature (Table I).

Thus, although S_c is finite at the estimated MCT T_c, S_{c2} vanishes at T_{K2} which coincides with T_c.

V. ANALYTICAL RESULTS

Our study shows that the AG theory, which is based on activation dynamics can completely describe the mode coupling theory power law behavior in the region where the latter is found to be valid (Fig. 2). However, the microscopic picture for mode coupling theory and the Adam Gibbs relation is different. Either from the heuristic arguments of Adam and Gibbs, or from the Random First Order Transition (RFOT) derivation, the AG relation is obtained from an activation picture of the dynamics, whereas the MCT does not correspond to activated dynamics. This leads to the question of the role of entropy in MCT which will be the focus of this section.

A. Entropy and MCT

In the $k \to 0$ limit, the memory function for a monatomic system, $\mathcal{M}(k,t)$ can be written as

$$\mathcal{M}(k,t) = \frac{S(k)}{8\pi^2\rho k}\int_0^\infty dq \times q^2(S(q)-1)^2 \times \phi^2(q,t). \tag{17}$$

In the schematic MCT, the $\phi(q,t)$ is usually decoupled from q and the rest of the memory function is integrated over the first peak of the S(q). The coupling constant λ is then considered to be proportional to this integrated value. This decoupling is possible as the dominant contribution in the memory function comes from the first peak of S(q).[57,58] Here, we consider a similar decoupling; however, we do not restrict ourself to first peak of S(q). Thus, we write Eq. (17) as

$$\mathcal{M}(k,t) = \frac{S(k)}{4\rho k(2\pi)^3}\left[\int_0^\infty d\mathbf{q}(S(q)-1)^2\right] \times \phi^2(k,t). \tag{18}$$

By writing S(q) in terms of g(r), we can rewrite Eq. (18) as

$$\mathcal{M}(k,t) = \frac{S(k)}{2k} \times 2\pi\rho\left[\int dr r^2(g(r)-1)^2\right]\phi^2(k,t). \tag{19}$$

In Eq. (9), we replace $\mathcal{M}(k,t)$ by its approximate form given in Eq. (19). Considering over damped limit and also by omitting the explicit "k" dependence of $\phi(t)$, Eq. (9) can be written in

schematic form as

$$\dot{\phi}(t) + \Omega^2\phi(t) + \Omega^2\lambda \int_0^t dt'\phi^2(t')\dot{\phi}(t-t') = 0, \quad (20)$$

where now we can identify the coupling parameter λ as

$$\lambda = \frac{S(k)}{2k} \times 2\pi\rho \int dr r^2 (g(r)-1)^2 = -\frac{S(k)}{2k}\frac{S_{2approx}}{k_B}. \quad (21)$$

Here, we call $S_{2approx}$ as the approximate pair entropy. Note that similar analysis can be extended to a binary system and $S_{2approx}$ can be written as

$$\frac{S_{2approx}}{k_B} = -2\pi\rho \sum_{\alpha,\beta} x_\alpha x_\beta \int_0^\infty dr r^2 [g_{\alpha\beta}(r)-1]^2. \quad (22)$$

The choice of calling it entropy will become clear in the next analysis. Note that although we do the derivation for a single component system the numerical calculations are all done for binary mixtures.

Our numerical analysis shows that for all the systems studied here, $S_{2approx}$ vs S_2 is indeed linear (Fig. 4) with a slope = 2.5.

To understand this proportionality, we expand the logarithmic term of Eq. (13) for $g_{\alpha\beta}(r) > 0$,

$$\frac{S_2}{k_B} = -2\pi\rho \sum_{\alpha,\beta} \int_0^\infty dr r^2 [g_{\alpha\beta}(r)-1]^2 \frac{1}{(g_{\alpha\beta}(r)+1)} + H, \quad (23)$$

where in "H" we put the higher order contributions. The Fig. 5 shows that the primary contribution comes from the first term of Eq. (23).

In the above equation, we note that $r^2[g_{\alpha\beta}(r)-1]^2$ varies strongly compared to $1/(g_{\alpha\beta}(r)+1)$. In the latter, if we consider $g_{\alpha\beta}(r) \approx 1$ we can write

$$\frac{S_{2approx}}{k_B} = -2\pi\rho \sum_{\alpha,\beta} \int_0^\infty dr r^2 [g_{\alpha\beta}(r)-1]^2 \sim 2\frac{S_2}{k_B} - 2H. \quad (24)$$

Thus, analytically we can predict the value of the slope to be 2. But this is a limiting case. For the systems studied here, near the peaks, $g_{\alpha\beta}(r)$ has values greater than 1. Hence the value of the slope is expected to be greater than 2 which supports the numerical observation.

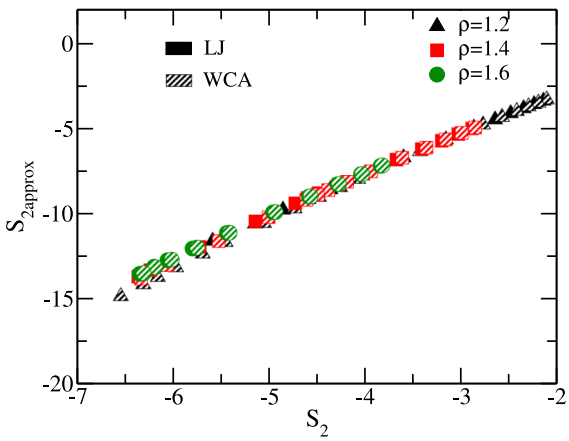

FIG. 4. $S_{2approx}$ is plotted against S_2 and it shows a linear behaviour with a slope ≈ 2.5.

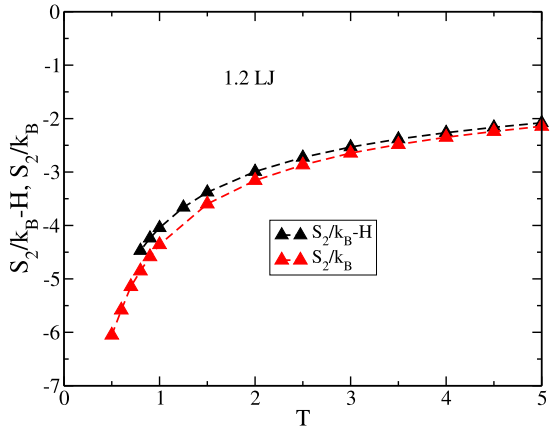

FIG. 5. The function ($\frac{S_2}{k_B} - H$) of Eq. (23) and S_2/k_B is plotted as a function of temperature. The plot shows that the primary contribution comes from the first term of the expansion.

Thus, the coupling constant λ can be related to the pair entropy,

$$\lambda = -\frac{S(k)}{2k} \times \frac{S_{2approx}}{k_B} = -m_s \frac{S(k)}{2k}(S_2/k_B - H), \quad (25)$$

where m_s is the slope obtained from $S_{2approx}$ vs S_2 plot.

The MCT relaxation time from schematic model[58] is given by

$$\tau \sim (1 - \frac{\lambda}{4})^{-\gamma}. \quad (26)$$

Note that the power law behaviour of relaxation time τ (as given by Eq. (26)) changes to exponential dependence of τ under generalized MCT formalism,[59] when the coupling parameter is considered to be the same for all higher order terms and frequency $\Omega \sim 1$. With these conditions τ can be written as

$$\tau = \frac{1}{\Omega^2\lambda}(\exp(\lambda) - 1) \sim \frac{\exp(\lambda)}{\lambda} \sim C'\exp(K'S_2). \quad (27)$$

The second equality is written by replacing λ from Eq. (25). Where C' and K' are not constants, they rather have a temperature dependence.

Earlier study of diffusion[24] and our present microscopic derivation of the Rosenfeld relation for relaxation time τ show that similar to Rosenfeld prediction, the MCT also predicts it to be a universal scaling law for all transport coefficients.

VI. NUMERICAL RESULTS

A. Rosenfeld scaling and MCT

In this section, we analyze the MCT results in the light of Rosenfeld relation. We find that the relaxation time as obtained from microscopic MCT, τ_{MCT} when plotted against λ does not follow the power law ($(1 - \frac{\lambda}{4})^{-\gamma}$) or $\exp(\lambda)$ dependence in the whole temperature regime. Note that only very close to the transition temperature, the power law behaviour is expected to be valid.[45] However, surprisingly we find that $\ln(\lambda\tau_{MCT})$ vs λ follows a linear behaviour (Fig. 6(a)), where the τ_{MCT} has been calculated only at the two body level, whereas the exponential dependence comes when higher order correlations are considered.

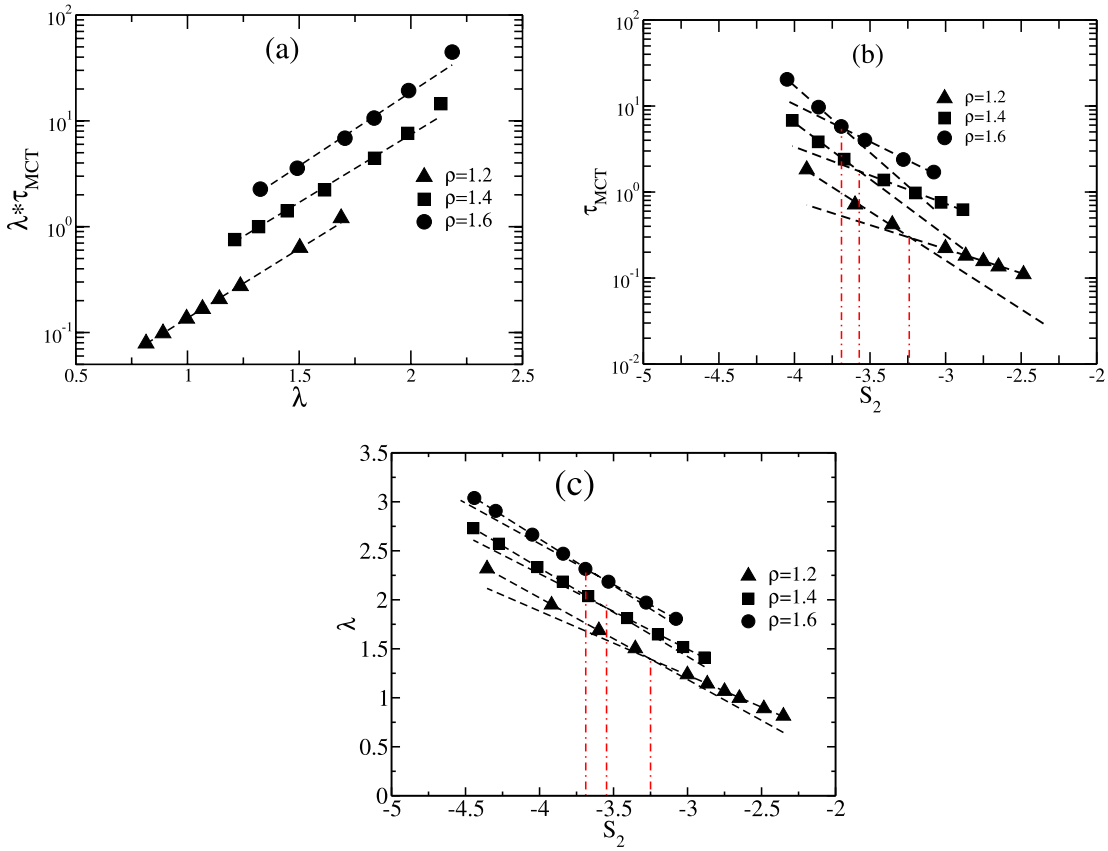

FIG. 6. (a) The plot of $\ln(\lambda\tau_{MCT})$ vs λ shows a linear regime for wide temperature range. (b) The relaxation times obtained from microscopic MCT, τ_{MCT} are plotted against S_2. The dashed lines illustrate the two different Rosenfeld regimes. (c) Plot of λ vs. S_2 also shows two different linear regimes. For clarity $\ln(\lambda\tau_{MCT})$ and $\ln(\tau_{MCT})$ are shifted by 1.0 and 2.0 and for λ it is −0.2 and −0.48 for the systems of $\rho = 1.4$ and $\rho = 1.6$, respectively. The breaks in the slope for both the plots are illustrated by vertical dashed-dotted lines. We show that for a fixed density the breaks for both τ_{MCT} and λ are at the same S_2 value.

Usually it is found[21,25] that both τ_{MCT} and τ (relaxation time obtained from simulation) when plotted against S_2 do not show a single straight line. For τ_{MCT}, the Rosenfeld break happens at high temperature compared to simulation data and these can be attributed to the well known difference in microscopic MCT transition temperature and T_c.[45,55] In Fig. 6(b), we plot the τ_{MCT} calculated from Eq. (11) against S_2 and similar to earlier studies it shows two linear regimes. The origin of this break or the temperature dependence of the Rosenfeld parameters "C'" and "K'" is not known in the literature.

Our analysis of Eq. (25) shows that the Rosenfeld parameters are related to the static structure factor $S(k)$. Thus, the temperature dependence of $S(k)$ leads to the temperature dependence of Rosenfeld parameters "C'" and "K'." However, since $S(k)$ changes continuously with temperature, it should lead to a similar temperature dependence of "C'" and K'. When we plot λ against S_2 we find that continuously changing values for "C'" and "K'" are not needed to describe the observed behaviour but two distinct values suffice (Fig. 6(b)). We see that there is a break in the slope and it happens at the same S_2 value where τ against S_2 shows a break in slope.

Next, we show that the value of $S_{2approx}$ and its temperature dependence as compared to S_{ex} can explain (i) the larger values of τ_{MCT} as compared to τ[45] and (ii) the higher values of activation energy as predicted by MCT.[4] Note that, in an earlier study, the activation energy E_0, for the simulated system was calculated from the time scale of self-intermediate scattering function, whereas for the MCT part, it was calculated from the time scale of intermediate scattering function.[4] We have followed a similar prescription. E_0^{sim} and E_0^{MCT}, as shown in Table II, are obtained by fitting τ and τ_{MCT} to Arrhenius expression,

$$\tau \sim \tau_0 \exp \frac{E_0}{T}. \tag{28}$$

Fig. 7 shows that at all densities for both the systems $S_{2approx}$ are smaller than S_{ex} and has a much stronger temperature dependence. Using Rosenfeld Expression, we can write

TABLE II. E_0 values are tabulated for different systems. We show that the E_0 values are higher for MCT as well as for approximate calculation compared to that of simulation results. Note that in an earlier study the activation energy E_0 for the simulated system was calculated from $\phi_s(q,t)$, whereas for the MCT part, it was calculated from $\phi(q,t)$.[4] We have followed a similar prescription.

	$\rho = 1.2$		$\rho = 1.4$		$\rho = 1.6$	
	LJ	WCA	LJ	WCA	LJ	WCA
E_0^{sim}	2.509	1.901	5.997	5.694	12.499	11.749
E_0^{MCT}	5.002	3.993	11.565	10.775	21.748	21.082
E_0^{approx}	6.224	5.705	16.535	15.831	37.159	36.564

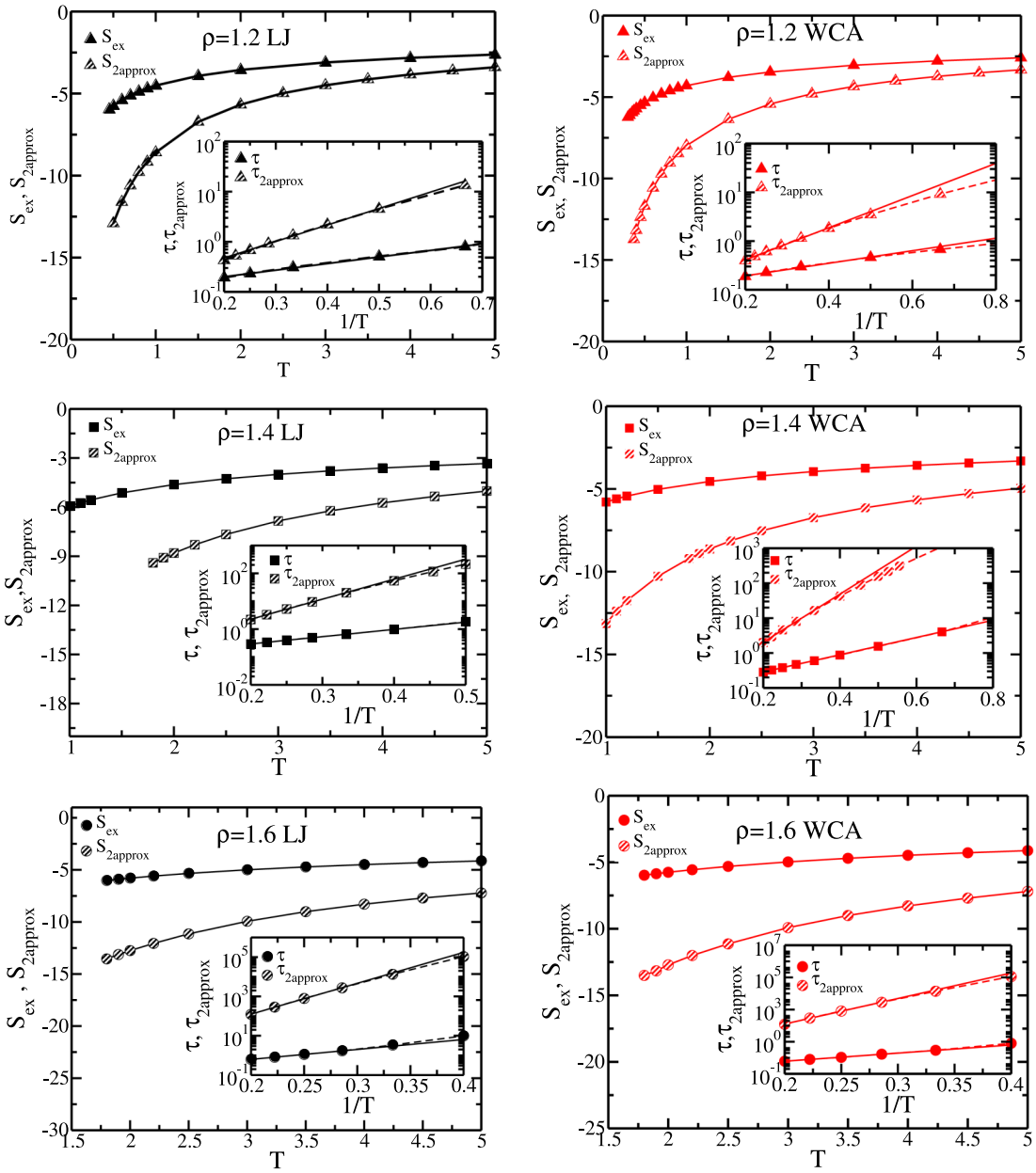

FIG. 7. S_{ex} and $S_{2approx}$ are plotted as a function of temperature for LJ and WCA systems at densities 1.2, 1.4, and 1.6. For all the systems $S_{2approx}$ has stronger temperature dependence and has smaller value than S_{ex}. In inset we plot $\tau_{2approx}$ as obtained from Eq. (30). It shows that $\tau_{2approx}$ has higher value and a larger slope leading to higher activation energy as compared to τ. Activation energies are tabulated in Table II.

$$\tau(T) = C \exp(-K S_{ex}). \tag{29}$$

Now if we replace S_{ex} by $S_{2approx}$, keeping C and K same, we get

$$\tau_{2approx} = C \exp(-K S_{2approx}). \tag{30}$$

The C and K are obtained from linear fits of logarithm of simulated relaxation time against excess entropy. Since $S_{2approx} \ll S_{ex}$, the study shows that $\tau_{2approx} \gg \tau$. The study also shows that similar to that predicted by microscopic MCT (Eq. (9)), the E_0 values for $\tau_{2approx}$ are higher, which are given in Table II.

Although the results obtained from $\tau_{2approx}$ shows the correct trend, it cannot match the parameters as obtained from τ_{MCT}. We note that the $\tau_{2approx}$ is a prediction obtained from schematic MCT, which is known to overestimate the coupling constant λ. However, this analysis not only explains the behaviour of MCT at high temperature, it also throws some light in the origin of its breakdown at low temperature. Usually the breakdown of MCT at low temperature has been attributed to the neglect of higher order correlation functions.[59,60] This present analysis predicts that the stronger temperature dependence of the vertex might be partially responsible for the breakdown of MCT even at low temperature.

B. The Adam Gibbs relation and MCT

We have shown that the relaxation time, τ, over a temperature regime ($10^{-1} \leq (\frac{T}{T_c} - 1) \leq 10^{0}$) follows both the AG relation and MCT power law behaviour. We also find that the avoided divergence observed in the configurational entropy plot (Fig. 2) arises from the vanishing of the pair

configurational entropy (S_{c2}). For all the systems studied here, we find $T_{K2} \simeq T_c$ (Table I). Note that although we find a strong empirical evidence for the coincidence of these two temperatures, we have not established a causal relationship between the vanishing of S_{c2} and MCT crossover. However, the AG theory, which describes activated motion, depends on the full S_c which has contributions both from pair and higher order correlations. Since activation is a many body effect, one may speculate that the pair contribution even in AG describes non-activated dynamics. Thus, it is plausible that similar to MCT T_c, the temperature at which S_{c2} goes to zero also marks a transition from non-activated to activated dynamics. Using the information given in Table I we can rewrite Eq. (16) as

$$TS_{c2} = K_{T2}\left(\frac{T}{T_{K2}} - 1\right) \simeq K_{T2}\left(\frac{T}{T_c} - 1\right). \tag{31}$$

We note that although $T_{K2} \simeq T_c$ and the MCT framework which predicts the power law behaviour is developed at the two body level, the AG relation with S_{c2} alone cannot predict the MCT power law behaviour. The RMPE plays an important role in predicting it. We also show that there is indeed a relation between MCT critical exponent γ, Adam Gibbs coefficient A, and the pair thermodynamic fragility K_{T2}.

As shown earlier in Eq. (12), configurational entropy can be written in terms of pair configurational entropy and RMPE. Thus, we can write

$$\frac{A}{TS_c} = \frac{A}{TS_{c2} + T\Delta S} = \frac{A}{K_{T2}} \frac{1}{[(\frac{T}{T_c} - 1) + \frac{T\Delta S}{K_{T2}}]}, \tag{32}$$

where we have used Eqs. (12) and (31) to write the first and second equalities, respectively.

We find that although $T\Delta S$ is system dependent (Fig. 8(a)), except for WCA system at $\rho = 1.2$, the function $\frac{T\Delta S}{K_{T2}}$ shows a master plot when plotted against $(\frac{T}{T_c} - 1)$ (Fig. 8(b)). Note that although the value of $\frac{T\Delta S}{K_{T2}}$ is small, it is not negligible.

The master plot of $\frac{T\Delta S}{K_{T2}}$ can be fitted to a straight line, $\frac{T\Delta S}{K_{T2}} = 0.26 - 0.35(\frac{T}{T_c} - 1)$. Next, we show that a function $\frac{1}{(\frac{T}{T_c} - 1) + f(T)}$, when plotted against $\ln(\frac{T}{T_c} - 1)$ shows linearity in the whole regime of $(10^{-1} \leq (\frac{T}{T_c} - 1) \leq 10^{0})$ only when $f(T)$ is non-negligible positive quantity (Fig. 8(c)). Note that in Fig. 8(c), when $f(T) = 0$ (which implies $\Delta S = 0$ in Eq. (32)), the function diverges strongly. This shows that the AG relation at two body level cannot predict the MCT power law behaviour.

The analysis further shows that to obtain a correct estimation of the MCT power law exponent γ (slope of the plot), $f(T)$ needs to obey the following temperature dependence, $f(T) = \frac{T\Delta S}{K_{T2}} = 0.26 - 0.35(\frac{T}{T_c} - 1)$. The two functions $\frac{T\Delta S}{K_{T2}}$ and

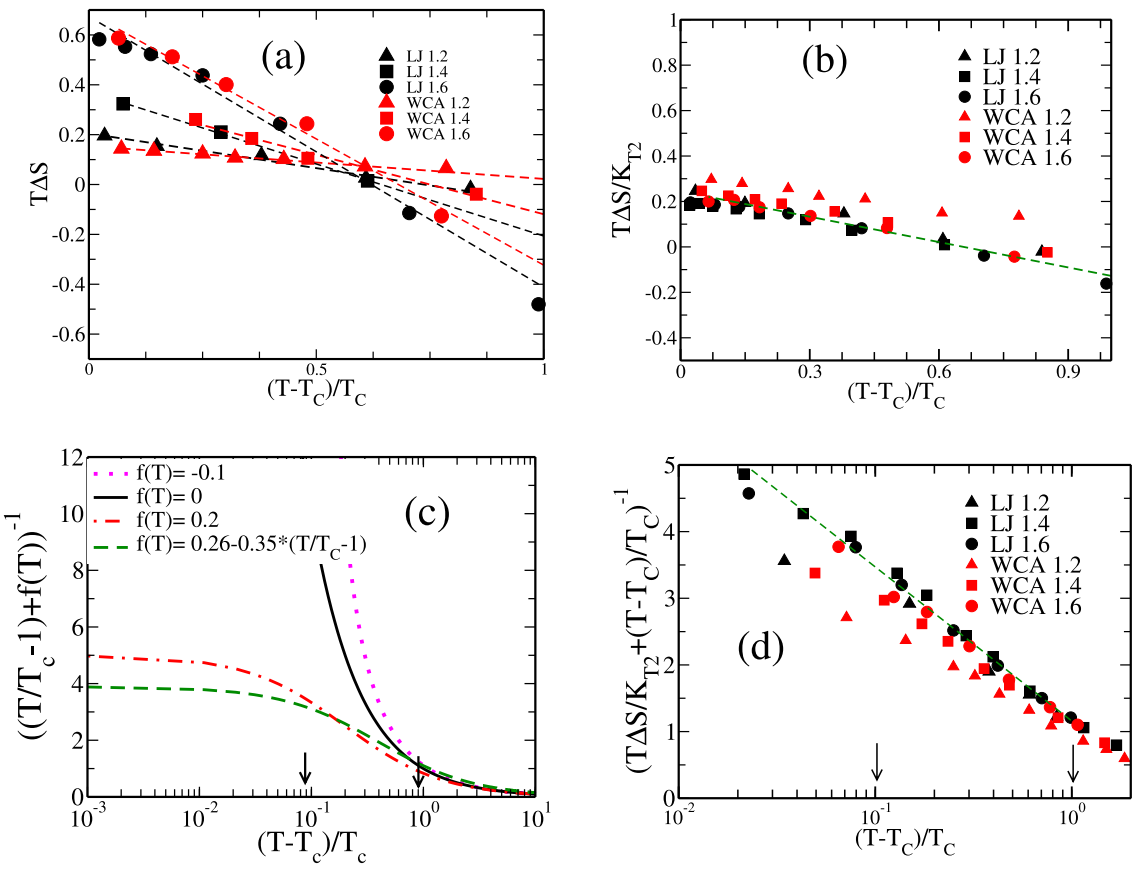

FIG. 8. (a) $T\Delta S$ values are plotted as a function of $(\frac{T}{T_c} - 1)$ and they show a strong system dependence. (b) $\frac{T\Delta S}{K_{T2}}$ vs $(\frac{T}{T_c} - 1)$ showing a master plot for all the systems except for WCA system at $\rho = 1.2$. Dotted line is guide to eye. (c) $((\frac{T}{T_c} - 1) + f(T))^{-1}$ plotted against $(\frac{T}{T_c} - 1)$ by varying $f(T)$. Only for non-negligible positive values of $f(T)$, linearity is found in the regime 0.1 to 1.0 of $(\frac{T}{T_c} - 1)$. To obtain a correct estimation of the MCT power law exponent γ (slope of the plot), f(T) needs to be temperature dependent (green dashed line). (d) $[\frac{1}{(\frac{T}{T_c} - 1) + \frac{T\Delta S}{K_{T2}}}]$ vs $(\frac{T}{T_c} - 1)$ shows a master plot for all the systems except for WCA system at $\rho = 1.2$. "m" is the slope of the linear plot which is tabulated in Table III.

TABLE III. The slope of the linear plot of $[\frac{1}{(\frac{T}{T_c}-1)+\frac{T\Delta S}{K_{T2}}}]$ vs $(\frac{T}{T_c}-1)$ in the region $(10^{-1} \le (\frac{T}{T_c}-1) \le 10^{0})$ (Fig. 8(a)).

ρ	$m(LJ)$	$m(WCA)$
1.2	0.987	0.749
1.4	1.038	0.888
1.6	1.004	1.000

$(\frac{T}{T_c}-1)$ contributing to the denominator in Eq. (32) show opposite trends, the former increases whereas the latter decreases with temperature. Therefore, a crossover between these two functions is observed in this regime. Around MCT transition temperature, $\frac{T\Delta S}{K_{T2}} \gg (\frac{T}{T_c}-1)$ and both the configurational entropy and the relaxation time are determined primarily by many body contributions.

From Fig. 8(d) we find in the temperature regime $(10^{-1} \le (\frac{T}{T_c}-1) \le 10^{0})$ Eq. (32) can be re-written as

$$\frac{A}{TS_c} = \frac{A}{K_{T2}} \frac{1}{[(\frac{T}{T_c}-1)+\frac{T\Delta S}{K_{T2}}]} \sim -\frac{mA}{K_{T2}} \ln(\frac{T}{T_c}-1), \tag{33}$$

where "m" is the slope obtained from Fig. 8(d) and given in Table III. Since τ is found to follow AG relation we can write

$$\tau \sim \exp(\frac{A}{TS_c}) \sim (\frac{T}{T_c}-1)^{\frac{mA}{K_{T2}}}. \tag{34}$$

Comparing Eqs. (14) and (34) we can write

$$\frac{mA}{K_{T2}} \sim \gamma, \tag{35}$$

where $m \simeq 1$ for all the systems except for the WCA system at $\rho = 1.2$. Thus, we show that the MCT scaling parameter, γ is related to the AG parameter, A and the pair thermodynamic fragility of S_{c2}, K_{T2}. We have tabulated the γ values in Table IV, which shows the above relation holds. The deviation of slope value ("m") from unity for WCA system at $\rho = 1.2$ may have some connection to its breakdown of density-temperature scaling which needs to be investigated in future.

The MCT critical exponent (γ) is known to be density-temperature independent[2]. Interestingly, we also find that although both AG coefficient (A) and pair thermodynamic fragility (K_{T2}) are strongly dependent on density and temperature (Table V), however their ratio, which is predicted here to be related to γ (Eq. (35)), is density-temperature independent (Table IV).

Note that there is an ambiguity in obtaining the MCT T_c and γ value. The fitted (empirical) mode-coupling temperature can be shifted quite a bit at the cost of changing the power law exponents. Whereas in the present calculation the T_{k2} and γ are obtained independently from two different fits. The T_{k2} is obtained from a linear fit (as shown in Fig. 3). Once T_{k2} is obtained, we can obtain the γ value by plotting $1/TS_c$ vs $\ln(\frac{T}{T_{k2}}-1)$, where the slope of the linear regime is related to γ (Eq. (15)). Thus, there is less ambiguity in obtaining T_{k2} and γ from entropy. Hence, we can consider T_{k2} as a less ambiguous quantity than T_c.

TABLE IV. mA/K_{T2} and γ for LJ and WCA system. As predicted by Eq. (35) mA/K_{T2} values are similar to γ values obtained from free fitting (Fig. 1) for most of the systems.

	$\rho = 1.2$		$\rho = 1.4$		$\rho = 1.6$	
	mA/K_{T2}	γ	mA/K_{T2}	γ	mA/K_{T2}	γ
LJ	2.32	2.23	2.38	2.39	2.35	2.30
WCA	2.93	2.24	2.86	2.29	2.58	2.30

TABLE V. The Adam Gibbs coefficient "A," as obtained from the linear fit of τ vs $1/TS_c$ plot, and pair thermodynamic fragility K_{T2}, as obtained from the linear fit of TS_{c2} vs T/T_{k2} plot for both the systems at different densities are tabulated below. The data show that both are strongly dependent on density.

ρ	$A(LJ)$	$A(WCA)$	$K_{T2}(LJ)$	$K_{T2}(WCA)$
1.2	1.87	1.89	0.795	0.483
1.4	3.57	4.37	1.555	1.358
1.6	6.96	7.57	2.971	2.936

VII. CONCLUSION

In this work, we show that in a certain region $(10^{-1} \le (\frac{T}{T_c}-1) \le 10^{0})$ the relaxation time follows both the AG relation and MCT power law behaviour. We also find that the MCT divergence temperatures coincide with the temperatures where pair configurational entropy goes to zero for all the systems studied here. AG relation is based on activated dynamics, whereas MCT is mean field theory which at the two body level does not address any activated dynamics. Also the microscopic MCT does not have any apparent connection to entropy. Thus, to understand the above mentioned observations, we explore the connection between mode coupling theory and entropy and discuss different predictions of MCT in the light of entropy.

We show that the MCT vertex for the structural relaxation time under certain approximations can be related to the pair excess entropy. Higher order MCT calculations in the schematic MCT framework can relate the relaxation time to the exponential of this vertex. Thus, the MCT can provide a microscopic derivation of the phenomenological Rosenfeld theory. Our analysis shows that the Rosenfeld parameters are related to the static structure factor $S(k)$. The temperature dependence of $S(k)$ leads to the temperature dependence of Rosenfeld parameters "C" and "K," thus explaining the earlier observation of the non-uniqueness of the Rosenfeld exponent.[25,26] The analysis of the vertex reveals that quantity which contributes to the vertex, $S_{2approx}$ has a much lower value and stronger temperature dependence as compared to the excess entropy, S_{ex}. If we assume the Rosenfeld scaling to be valid and replace S_{ex} by $S_{2approx}$, the predicted relaxation time shows similar characteristics as the MCT relaxation time. Thus, the study reveals that the larger value of τ_{MCT} and its higher activation energy as compared to the simulation results, is related to the value and temperature dependence of the vertex. This analysis further reveals that the breakdown of MCT at low temperature might be partially related to the strong temperature dependence of the vertex.

As mentioned earlier, the AG theory, which is based on activation dynamics, can completely describe the MCT power law behavior in the region where the latter is found to be valid. Since the configurational entropy has a finite value at the MCT

transition temperature, T_c, the AG relation is not expected to predict any avoided transition in this regime. Our study reveals that although S_c is finite, S_{c2} vanishes at T_{K2} (where $T_{K2} = T_c$), thus being responsible for the divergence like behavior. However, a causal relationship between the MCT crossover and vanishing of the pair configurational entropy is an open question to be addressed in the future. We also show that although the pair configurational entropy predicts the correct MCT transition temperature, it cannot, by itself, predict the MCT power law behaviour. The RMPE plays an important role in providing the correct temperature dependence of relaxation time. We also obtain a connection between the AG coefficient (A), pair thermodynamic fragility (K_{T2}), and MCT critical exponent (γ). The study shows that although first two quantities are dependent on density and temperature, their ratio, which is related to γ, is density-temperature independent.

Note that although the absolute value of ΔS is in the similar range both at high and low temperature regimes, in the high temperature regime it plays a minor role in determining the dynamics, whereas its role at low temperature becomes central as we approach the avoided transition. This small positive value of ΔS playing an important role in predicting the MCT power law behaviour is similar to the prediction of unified theory.[61] In the unified theory, it was shown that in a certain temperature regime many body activated dynamics plays a hidden but central role in predicting the MCT-like behaviour of the total relaxation time. Although apparently the MCT does not depend on the properties of landscape, the saddles in the landscape have been found to disappear at T_c.[62–65] Here, we show that S_{c2} also vanishes at T_c. Thus, there may be a connection between pair configurational entropy and saddles. It will be also interesting to understand the independent role of pair configurational entropy and RMPE in the landscape picture. These are also the important open questions to be addressed in the future work.

ACKNOWLEDGMENTS

This work has been supported by the Department of Science and Technology (DST), India and CSIR-Multi-Scale Simulation and Modeling project. M.K.N. thanks UGC and A.B. thanks DST for fellowships. The authors thank Biman Bagchi, Kunimasa Miyazaki and Walter Kob for discussions. We thank Mr. Sudip Sasmal for critical reading of the manuscript.

[1]W. Götze and L. Sjögren, Z. Phys. B: Condens. Matter **65**, 415 (1987).
[2]W. Götze, J. Phys.: Condens. Matter **11**, A1 (1999).
[3]L. Berthier and G. Tarjus, Phys. Rev. Lett. **103**, 170601 (2009).
[4]L. Berthier and G. Tarjus, Phys. Rev. E **82**, 031502 (2010).
[5]L. Berthier and G. Tarjus, Eur. Phys. J. E **34**, 96 (2011).
[6]L. Berthier and G. Tarjus, J. Chem. Phys. **134**, 214503 (2011).
[7]D. Coslovich, J. Chem. Phys. **138**, 12A539 (2013).
[8]D. Coslovich, Phys. Rev. E **83**, 051505 (2011).
[9]D. Kivelson, S. A. Kivelson, X. Zhao, Z. Nussinov, and G. Tarjus, Phys. A: Stat. Mech. Appl. **219**, 27 (1995).
[10]S. Karmakar and I. Procaccia, Phys. Rev. E **86**, 061502 (2012).
[11]A. Malins *et al.*, J. Chem. Phys. **138**, 12A535 (2013).
[12]G. M. Hocky, T. E. Markland, and D. R. Reichman, Phys. Rev. Lett. **108**, 225506 (2012).
[13]A. Banerjee, S. Sengupta, S. Sastry, and S. M. Bhattacharyya, Phys. Rev. Lett. **113**, 225701 (2014).
[14]Y. Rosenfeld, Phys. Rev. E **62**, 7524 (2000).
[15]G. Adam and J. H. Gibbs, J. Chem. Phys. **43**, 139 (1965).
[16]Y. Rosenfeld, J. Phys.: Condens. Matter **11**, 5415 (1999).
[17]I. Borzsk and A. Baranyai, Chem. Phys. **165**, 227 (1992).
[18]M. Dzugutov, Nature **381**, 6578 (1996).
[19]J. J. Hoyt, M. Asta, and B. Sadigh, Phys. Rev. Lett. **85**, 594 (2000).
[20]J. Mittal, J. R. Errington, and T. M. Truskett, J. Chem. Phys. **125**, 076102 (2006).
[21]R. Sharma, S. N. Chakraborty, and C. Chakravarty, J. Chem. Phys. **125**, 204501 (2006).
[22]R. Zwanzig, Proc. Natl. Acad. Sci. U. S. A. **85**, 2029 (1988).
[23]S. Banerjee, R. Biswas, K. Seki, and B. Bagchi, J. Chem. Phys. **141**, 124105 (2014).
[24]A. Samanta, S. M. Ali, and S. K. Ghosh, Phys. Rev. Lett. **87**, 245901 (2001).
[25]C. Kaur, U. Harbola, and S. P. Das, J. Chem. Phys. **123**, 034501 (2005).
[26]M. Agarwal, M. Singh, B. Shadrack Jabes, and C. Chakravarty, J. Chem. Phys. **134**, 014502 (2011).
[27]S. Sengupta, F. Vasconcelos, F. Affouard, and S. Sastry, J. Chem. Phys. **135**, 194503 (2011).
[28]S. Sengupta, S. Karmakar, C. Dasgupta, and S. Sastry, Phys. Rev. Lett. **109**, 095705 (2012).
[29]S. Mossa, E. La Nave, H. E. Stanley, C. Donati, F. Sciortino, and P. Tartaglia, Phys. Rev. E **65**, 041205 (2002).
[30]E. La Nave, A. Scala, F. W. Starr, F. Sciortino, and H. E. Stanley, Phys. Rev. Lett. **84**, 4605 (2000).
[31]E. La Nave, H. E. Stanley, and F. Sciortino, Phys. Rev. Lett. **88**, 035501 (2002).
[32]L. Berthier and D. Coslovich, Proc. Natl. Acad. Sci. U. S. A. **111**, 11668 (2014).
[33]R. Richert and C. A. Angell, J. Chem. Phys. **108**, 9016 (1998).
[34]L. M. Wang and R. Richert, Phys. Rev. Lett. **99**, 185701 (2007).
[35]F. Sciortino, W. Kob, and P. Tartaglia, Phys. Rev. Lett. **83**, 3214 (1999).
[36]S. Sastry, Nature **409**, 164 (2001).
[37]R. J. Speedy, J. Chem. Phys. **110**, 4559 (1999).
[38]R. J. Speedy, J. Chem. Phys. **114**, 9069 (2001).
[39]A. Angelani and G. Foffi, J. Phys.: Condens. Matter **19**, 256207 (2007).
[40]A. Scala, F. W. Starr, E. L. Nave, F. Sciortino, and H. E. Stanley, Nature (London) **406**, 166 (2000).
[41]F. W. Starr, S. Sastry, E. La Nave, A. Scala, H. Eugene Stanley, and F. Sciortino, Phys. Rev. E **63**, 041201 (2001).
[42]I. Saika-Voivod, F. Sciortino, and P. H. Poole, Phys. Rev. E **69**, 041503 (2004).
[43]S. Karmakar, C. Dasgupta, and S. Sastry, Proc. Natl. Acad. Sci. U. S. A. **106**, 3675 (2009).
[44]F. W. Starr, J. F. Douglas, and S. Sastry, J. Chem. Phys. **138**, 12A541 (2013).
[45]E. Flenner and G. Szamel, Phys. Rev. E **72**, 031508 (2005).
[46]W. Kob and H. C. Andersen, Phys. Rev. E **51**, 4626 (1995).
[47]J. D. Weeks, D. Chandler, and H. C. Andersen, J. Chem. Phys. **54**, 5237 (1971).
[48]S. J. Plimpton, J. Comput. Phys. **117**, 1 (1995).
[49]S. Sastry, Phys. Rev. Lett. **85**, 590 (2000).
[50]J. G. Kirkwood and E. M. Boggs, J. Chem. Phys. **10**, 394 (1942).
[51]R. E. Nettleton and M. S. Green, J. Chem. Phys. **29**, 1365 (1958).
[52]H. J. Raveché, J. Chem. Phys. **55**, 2242 (1971).
[53]D. C. Wallace, J. Chem. Phys. **87**, 2282 (1987).
[54]P. V. Giaquinta and G. Guinta, Physica A **187**, 145 (1992); S. Prestipino and P. V. Giaquinta, J. Stat. Phys. **96**, 135 (1999); F. Saija, S. Prestipino, and P. V. Giaquinta, J. Chem. Phys. **113**, 2806 (2000); **124**, 244504 (2006).
[55]Y. Brumer and D. R. Reichman, Phys. Rev. E **69**, 041202 (2004).
[56]A. Banerjee, S. Sastry, and S. M. Bhattacharyya, "Effect of structure and entropy in determining the dynamics of supercooled liquids: A density dependent study" (unpublished).
[57]U. Bengtzelius, W. Gotze, and A. Sjolander, J. Phys. C: Solid State Phys. **17**, 5915 (1984).
[58]E. Leutheusser, Phys. Rev. A **29**, 2765 (1984).
[59]L. M. C. Janssen, P. Mayer, and D. R. Reichman, Phys. Rev. E **90**, 052306 (2014).
[60]G. Szamel, Phys. Rev. Lett. **90**, 228301 (2003).
[61]S. M. Bhattacharyya, B. Bagchi, and P. G. Wolynes, Proc. Natl. Acad. Sci. U. S. A. **105**, 16077 (2008).
[62]L. Angelani, R. Di Leonardo, G. Ruocco, A. Scala, and F. Sciortino, Phys. Rev. Lett. **85**, 5356 (2000).
[63]L. Angelani, R. Di Leonardo, G. Ruocco, A. Scala, and F. Sciortino, J. Chem. Phys. **116**, 10297 (2002).
[64]J. P. K. Doye and D. J. Wales, J. Chem. Phys. **118**, 5263 (2003).
[65]L. Angelani, R. Di Leonardo, G. Ruocco, A. Scala, and F. Sciortino, J. Chem. Phys. **118**, 5265 (2003).